Phase diagram of the spin-Peierls chain with local coupling: Density-matrix renormalization-group calculations and unitary transformations

Alexander Weiße,[1] Georg Hager,[2] Alan R. Bishop,[3] and Holger Fehske[1]
[1]*Institut für Physik, Ernst-Moritz-Arndt-Universität Greifswald, Domstraße 10a, 17487 Greifswald, Germany*
[2]*Regionales Rechenzentrum Erlangen, HPC Services, Martensstraße 1, 91058 Erlangen, Germany*
[3]*Los Alamos National Laboratory, Los Alamos, New Mexico 87545, USA*
(Received 7 July 2006; revised manuscript received 30 October 2006; published 27 December 2006)

We explore the ground-state phase diagram of a Heisenberg spin chain coupled locally to optical phonons (bond coupling), using large-scale density-matrix renormalization-group calculations and extending a unitary transformation approach which removes the spin-phonon coupling in leading order. For the quantum phase transition from the spin liquid to the dimerized phase, we find deviations from previous quantum Monte Carlo and flow equation results.

DOI: 10.1103/PhysRevB.74.214426 PACS number(s): 75.10.Pq, 63.70.+h, 71.38.−k

I. INTRODUCTION

The interaction of electronic and lattice degrees of freedom in combination with reduced dimensionality can lead to a variety of interesting effects, one of which is the instability of a one-dimensional metal toward lattice distortion and the opening of a gap at the Fermi surface that was first described by Peierls.[1] A similar effect is observed in quantum spin chains, where the coupling to the lattice can cause a transition from a spin liquid with gapless excitations to a dimerized phase with an excitation gap. Experimentally such behavior was first observed in the 1970s for organic compounds of the TTF (tetrathiofulvalene) and TCNQ (tetracyanoquinodimethan) family,[2] but the topic regained attention after the discovery of the first inorganic spin-Peierls compound $CuGeO_3$ in 1993 by Hase *et al.*[3] In this material Cu^{2+} ions form well separated spin-1/2 chains with an exchange interaction that couples to high-frequency optical phonons ($\omega \approx J$), and the phonon dynamics at the phase transition is governed by a central peak rather than a soft-mode behavior.[4–9] These features distinguish $CuGeO_3$ from other spin-Peierls systems and sparked the interest in a nonadiabatic modeling.

A good starting point is the study of simplified microscopic models, which can be built from three ingredients,

$$H = H_s + H_p + H_{sp}. \tag{1}$$

Here $H_s = \Sigma_i \vec{S}_i \cdot \vec{S}_{i+1}$ and $H_p = \omega \Sigma_i b_i^\dagger b_i$ describe a Heisenberg spin-1/2 chain and a set of harmonic (Einstein) oscillators which are coupled by an interaction term H_{sp}. For this interaction we can consider two simple forms,

$$H_{sp}^{\mathrm{diff}} = g\omega \sum_i (b_i^\dagger + b_i)(\vec{S}_i \cdot \vec{S}_{i+1} - \vec{S}_{i-1} \cdot \vec{S}_i), \tag{2}$$

and

$$H_{sp}^{\mathrm{loc}} = g\omega \sum_i (b_i^\dagger + b_i)\vec{S}_i \cdot \vec{S}_{i+1}. \tag{3}$$

The first type of spin-phonon interaction, H_{sp}^{diff}, has been studied with a number of methods, including perturbation theory,[10,11] flow equations,[12,13] exact diagonalization,[11] and density matrix renormalization-group (DMRG).[14,15] The latter approach identified the ground-state phase diagram, but also analytically the quantum phase transition from the gapless to the dimerized phase is rather well understood: For finite phonon frequency ω the spin-phonon coupling g leads to effective spin interactions beyond nearest-neighbor exchange, i.e., the low energy physics is governed by a frustrated Heisenberg model. As we know from the spin model

$$H = \sum_i (\vec{S}_i \cdot \vec{S}_{i+1} + \alpha \vec{S}_i \cdot \vec{S}_{i+2}), \tag{4}$$

frustration can lead to dimerization if the parameter α exceeds a certain critical value ($\alpha_c = 0.241\,167$ in this case[16–18]), and similarly we obtain a finite $g_c(\omega)$.[11,12,14,15]

For the second type of spin-phonon coupling, H_{sp}^{loc}, which applies to $CuGeO_3$, to date the precise location of the phase boundary was arguable. In previous studies[11,23] we calculated g_c using perturbation theory, a variational ansatz, as well as exact diagonalization of small systems. This was challenged by results of the flow equation method and, in a limited parameter range, by quantum Monte Carlo.[19,24] In this article we present unbiased results of large-scale DMRG calculations, and extend our perturbation theory by several orders in g, high enough to ensure convergence. The results are summarized in Fig. 1 and compared to other approaches. More details now follow.

II. NUMERICAL RESULTS

DMRG calculations are certainly the most precise numerical tool for studying the low energy properties of one-dimensional models, but as yet have only been performed for the spin-Peierls model with difference coupling[14] H_{sp}^{diff}, models with acoustic phonons,[25] or with XY-type spin interaction.[26] We therefore implemented the local spin-phonon interaction H_{sp}^{loc}, using a high-performance, parallel version of the usual two-block finite-lattice algorithm with up to 1000 states per block. To detect the quantum phase transition from the gapless to the dimerized phase we use the established criterion of the level-crossing between the first singlet and the first triplet excitation, which was derived for the frustrated spin chain,[27] Eq. (4), and has successfully been applied[14,15] in the case of H_{sp}^{diff}. For finite systems in the gapless phase the lowest singlet excitation is above the low-

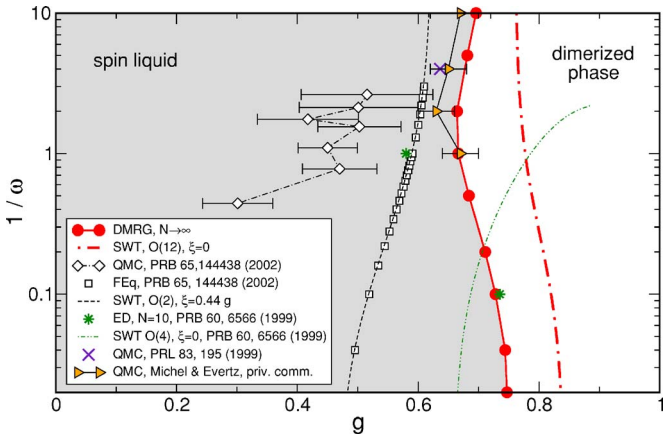

FIG. 1. (Color online) Ground-state phase diagram of the spin-Peierls chain with local coupling: QMC, flow equation (FEq) and exact diagonalization results (Refs. 11 and 19–22) compared to DMRG data and results of 12th order Schrieffer-Wolff transformation (SWT).

est triplet, both becoming degenerate with the singlet ground state for system size $N\to\infty$. In the gapped phase, for $N\to\infty$ the lowest singlet becomes degenerate with the ground state to form the symmetry-broken dimerized state, whereas the lowest triplet maintains a finite gap. Consequently, the two excitations will cross at the quantum critical point. Note however, that for small phonon frequency ω the relevant singlet excitation can be confused with a copy of the ground state plus an excited phonon. This frequency range therefore requires rather large N for the correct crossing to be detectable in the low energy spectrum of the spin-Peierls models.

In Fig. 2 we show the level difference as a function of the spin-phonon coupling for various system sizes and two typical phonon frequencies. For $\omega\gtrsim 0.5$ there is almost no finite-size dependence of the critical coupling g_c, whereas for smaller frequencies, the data scales noticeably. It is tempting to attribute this different behavior to the cross over from the antiadiabatic to the adiabatic regime, naïvely expected for $\omega\sim J\equiv 1$. However, as was pointed out in previous

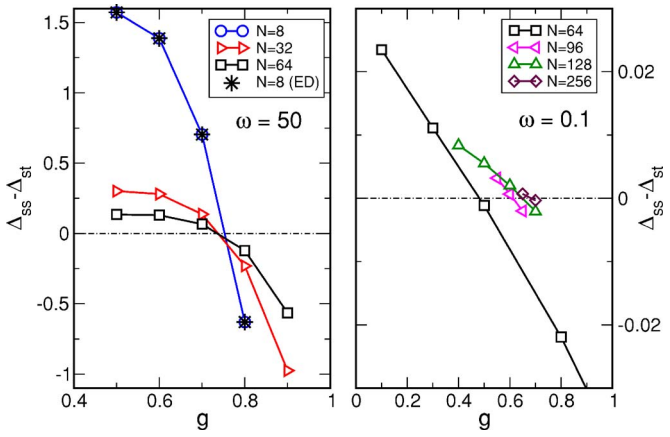

FIG. 2. (Color online) Crossing of the singlet and triplet gaps for large (left) and small (right) phonon frequency. Note the different finite-size scalings.

studies,[26,28,29] the relevant scale for the adiabatic to antiadiabatic cross over is given by the excitation gap, $\omega\sim\Delta$. The larger N dependence of g_c observed in Fig. 2 for $\omega=0.1$ is therefore related to the finite-size gap still being close ω, and will disappear for $N\to\infty$. Note also, that the bosonization[26,28,29] results support the analytical approach we present in the following, which is based on the assumption of antiadiabaticity.

III. ANALYTICAL RESULTS

Already in our earlier work[11] we suggested to construct an effective spin model for the low energy physics of the spin-Peierls problem by integrating out the phonons with a Schrieffer-Wolff transformation.[30] This removes the spin-phonon interaction in lowest order, and after averaging over the phonon vacuum yields an effective spin-only model. The approach is closely related to the Lang-Firsov transformation,[31] which is well known from polaron physics. In more detail, we apply the unitary transformation $\tilde{H}=\exp(S)H\exp(-S)$, where

$$S=g\sum_i (b_i^\dagger-b_i)\vec{S}_i\cdot\vec{S}_{i+1}. \tag{5}$$

Unfortunately, this transformation cannot be evaluated exactly, but needs to be approximated by an expansion in iterated commutators:

$$\tilde{H}=\sum_k [S,H]_k/k\,!\,, \tag{6}$$

where $[S,H]_{k+1}=[S,[S,H]_k]$ and $[S,H]_0=H$. For increasing expansion order these commutators quickly become very complicated and easily involve millions of terms. Using FORM,[32,33] an algebra tool popular in high energy physics, we are now able to push the limit of the expansion to order $k=12$, a tremendous advantage over our previous results with $k=4$. For the last step, we decided to be more general by averaging the transformed Hamiltonian over coherent states with $b_i|\xi\rangle=\xi|\xi\rangle$ instead of just the phonon vacuum:

$$H_{\text{eff}}=\langle\xi|\tilde{H}|\xi\rangle=J_0N+\sum_i\sum_{n=1}^{7}J_n\vec{S}_i\cdot\vec{S}_{i+n}+\text{multispin terms}. \tag{7}$$

This allows for a direct comparison with the flow equation result of Raas *et al.*,[19] which is equivalent to a second order expansion ($k=2$) with phonon shift $\xi=-\langle\vec{S}_i\cdot\vec{S}_{i+1}\rangle g\approx(1/4-\ln 2)g\approx 0.44g$. Here the spin correlator is approximated by its value in the isotropic Heisenberg chain. For a comparison see the small squares and the thin dashed line in Fig. 1.

In Table I we list the expansion coefficients of the resulting long-ranged exchange interactions J_n that contribute to our effective Hamiltonian Eq. (7). We neglect interactions that involve more than two spin operators. The phase transition line in Fig. 1 is obtained by equating the effective frustration $\alpha_{\text{eff}}=:J_2/J_1$ with the critical value α_c of the next-nearest-neighbor spin chain [see Eq. (4)]. This approximation is justified, because the J_n decay rapidly with increas-

TABLE I. Expansion of the effective long-ranged exchange $J_n\vec{S}_i\cdot\vec{S}_{i+n}$ in powers of the spin-phonon coupling g.

	J_0	J_1	J_2	J_3	J_4	J_5	J_6	J_7
g^0	$\xi^2\omega$	1						
g^2		$-\frac{1}{2}$	$\frac{1}{2}$					
$g^2\omega$	$-\frac{3}{16}$	$\frac{1}{2}$						
$g^3\xi\omega$		$-\frac{2}{3}$	$\frac{2}{3}$					
g^4		$\frac{7}{24}$	$-\frac{37}{96}$	$\frac{3}{32}$				
$g^4\omega$	$\frac{3}{64}$	$-\frac{3}{8}$	$\frac{3}{16}$					
$g^5\xi\omega$		$\frac{7}{15}$	$-\frac{37}{60}$	$\frac{3}{20}$				
g^6		$-\frac{697}{5760}$	$\frac{541}{2880}$	$-\frac{29}{384}$	$\frac{5}{576}$			
$g^6\omega$	$-\frac{1}{64}$	$\frac{29}{144}$	$-\frac{91}{576}$	$\frac{5}{192}$				
$g^7\xi\omega$		$-\frac{697}{3360}$	$\frac{541}{1680}$	$-\frac{29}{224}$	$\frac{5}{336}$			
g^8		$\frac{5119}{129024}$	$-\frac{88339}{1290240}$	$\frac{45749}{1290240}$	$-\frac{3685}{516096}$	$\frac{35}{73728}$		
$g^8\omega$	$\frac{107}{24576}$	$-\frac{3611}{46080}$	$\frac{3569}{46080}$	$-\frac{683}{30720}$	$\frac{35}{18432}$			
$g^9\xi\omega$		$\frac{5119}{72576}$	$-\frac{88339}{725760}$	$\frac{45749}{725760}$	$-\frac{3685}{290304}$	$\frac{35}{41472}$		
g^{10}		$-\frac{2516207}{232243200}$	$\frac{9363217}{464486400}$	$-\frac{105569}{8601600}$	$\frac{171601}{51609600}$	$-\frac{7601}{19353600}$	$\frac{7}{409600}$	
$g^{10}\omega$	$-\frac{18101}{17203200}$	$\frac{35017}{1433600}$	$-\frac{72439}{2580480}$	$\frac{1243}{115200}$	$-\frac{42433}{25804800}$	$\frac{7}{81920}$		
$g^{11}\xi\omega$		$-\frac{2516207}{127733760}$	$\frac{9363217}{255467520}$	$-\frac{105569}{4730880}$	$\frac{171601}{28385280}$	$-\frac{691}{967680}$	$\frac{7}{225280}$	
g^{12}		$\frac{624432139}{245248819200}$	$-\frac{820409053}{163499212800}$	$\frac{62408713}{18166579200}$	$-\frac{138813341}{122624409600}$	$\frac{12753401}{70071091200}$	$-\frac{6906257}{490497638400}$	$\frac{77}{176947200}$
$g^{12}\omega$	$\frac{69371}{309657600}$	$-\frac{441857}{68812800}$	$\frac{1701589}{206438400}$	$-\frac{7128059}{1857945600}$	$\frac{280187}{348364800}$	$-\frac{4939}{66355200}$	$\frac{77}{29491200}$	
$g^{13}\xi\omega$		$\frac{624432139}{122624409600}$	$-\frac{820409053}{81749606400}$	$\frac{62408713}{9083289600}$	$-\frac{138813341}{61312204800}$	$\frac{12753401}{35035545600}$	$-\frac{6906257}{245248819200}$	$\frac{77}{88473600}$

ing n, as we illustrate in Fig. 3. For the phonon average we use $\xi=0$, which corresponds to the vacuum. Except for a rather small offset, the analytical result matches the DMRG data quite well. In particular, the slope of the critical line is captured correctly. Eventually the agreement could be improved with a further unitary transformation which removes the next order of the electron-phonon interaction. However, this is technically involved and out of reach so far.

The convergence of our analytical approach is illustrated in Fig. 4, depicting the phase transition lines obtained for increasing expansion order. We observe an oscillatory behavior, such that reliable data results only beyond order $k\geq 8$. For lower orders, α_{eff} may not even reach the critical value, as is evident from the order 6 data shown in the inset. Nevertheless, for order 6 the phase transition can be estimated using a Shanks transformation.[34]

We also checked, if the phonon shift $\xi\approx 0.44g$ proposed by Raas *et al.*[19] leads to an improved effective description, but clearly the dot-dashed line in Fig. 4 deviates qualitatively from the DMRG data. Within the flow equation approach this shift was motivated by the requirement for normal ordering such that the phonons couple to $(\vec{S}_i\cdot\vec{S}_{i+1}-\langle\vec{S}_i\cdot\vec{S}_{i+1}\rangle)$. Even though this appears natural and can be motivated on a

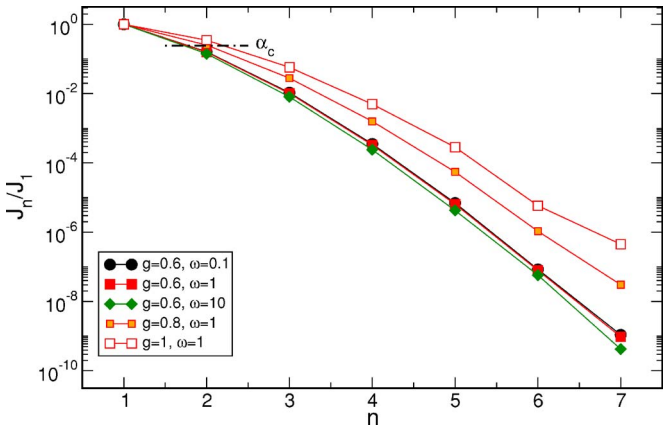

FIG. 3. (Color online) The effective Heisenberg coupling J_n decreases rapidly with the range n. Note the logarithmic scale.

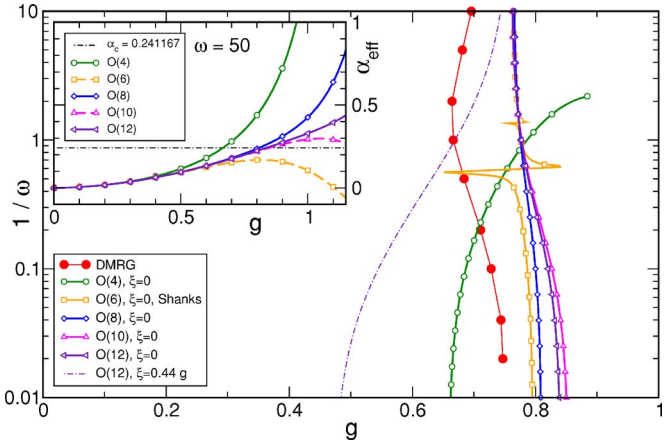

FIG. 4. (Color online) Convergence of the Schrieffer-Wolff approach with increasing expansion order $O(k)$. Main panel: phase diagram showing DMRG and expansion data for order 4–12 without and with oscillator shifts. Inset: α_{eff} as a function of g for $\omega = 50$ and orders 4–12.

mean field level, it does not seem to capture the important physics. This might be related to the strong coupling situation which we need to describe here.

IV. CONCLUSIONS

To summarize, using DMRG we obtained the, to date, most precise numerical result for the location of the quantum phase transition from the spin liquid to the dimerized phase in the one-dimensional Heisenberg model with local coupling to optical phonons. In addition, we proved the convergence of the unitary transformation approach that maps the full spin-phonon model to an effective frustrated spin model and allows an analytical calculation of the phase boundary in good agreement with the numerical data.

ACKNOWLEDGMENTS

We thank F. Michel and H. G. Evertz for providing their very recent QMC data and E. Jeckelmann and G. Wellein for many helpful comments. In addition, we acknowledge the generous grant of resources by HLRN and NERSC, and financial support by DFG through SPP 1073. Work at Los Alamos was performed under the auspices of the US DOE.

[1] R. Peierls, *Quantum Theory of Solids* (Oxford University Press, Oxford, 1955).
[2] J. W. Bray, H. R. Hart, Jr., L. V. Interrante, I. S. Jacobs, J. S. Kasper, G. D. Watkins, S. H. Wee, and J. C. Bonner, Phys. Rev. Lett. **35**, 744 (1975).
[3] M. Hase, I. Terasaki, and K. Uchinokura, Phys. Rev. Lett. **70**, 3651 (1993).
[4] M. Braden, B. Hennion, W. Reichardt, G. Dhalenne, and A. Revcolevschi, Phys. Rev. Lett. **80**, 3634 (1998).
[5] C. Gros and R. Werner, Phys. Rev. B **58**, R14677 (1998).
[6] H. Fehske, M. Holicki, and A. Weiße, in *Advances in Solid State Physics 40*, edited by B. Kramer (Vieweg, Wiesbaden, 2000), pp. 235–249.
[7] J.-P. Pouget, Eur. Phys. J. B **20**, 321 (2001).
[8] J.-P. Pouget, Eur. Phys. J. B **24**, 415 (2001).
[9] S. Trebst, N. Elstner, and H. Monien, Europhys. Lett. **56**, 268 (2001).
[10] K. Kuboki and H. Fukuyama, J. Phys. Soc. Jpn. **56**, 3126 (1987).
[11] A. Weiße, G. Wellein, and H. Fehske, Phys. Rev. B **60**, 6566 (1999).
[12] G. S. Uhrig, Phys. Rev. B **57**, R14004 (1998).
[13] C. Raas, A. Bühler, and G. S. Uhrig, Eur. Phys. J. B **21**, 369 (2001).
[14] R. J. Bursill, R. H. McKenzie, and C. J. Hamer, Phys. Rev. Lett. **83**, 408 (1999).
[15] G. Hager, A. Weiße, G. Wellein, E. Jeckelmann, and H. Fehske cond-mat/0606360, J. Magn. Magn. Mater. (to be published).
[16] K. Okamoto and K. Nomura, Phys. Lett. A **169**, 433 (1992).
[17] G. Castilla, S. Chakravarty, and V. J. Emery, Phys. Rev. Lett. **75**, 1823 (1995).
[18] S. Eggert, Phys. Rev. B **54**, R9612 (1996).
[19] C. Raas, U. Löw, G. S. Uhrig, and R. W. Kühne, Phys. Rev. B **65**, 144438 (2002).
[20] A. W. Sandvik, R. R. P. Singh, and D. K. Campbell, Phys. Rev. B **56**, 14510 (1997).
[21] A. W. Sandvik and D. K. Campbell, Phys. Rev. Lett. **83**, 195 (1999).
[22] F. Michel and H. G. Evertz (private communication).
[23] G. Wellein, H. Fehske, and A. P. Kampf, Phys. Rev. Lett. **81**, 3956 (1998).
[24] R. W. Kühne and U. Löw, Phys. Rev. B **60**, 12125 (1999).
[25] W. Barford and R. J. Bursill, Phys. Rev. Lett. **95**, 137207 (2005).
[26] L. G. Caron and S. Moukouri, Phys. Rev. Lett. **76**, 4050 (1996).
[27] I. Affleck, D. Gepner, H. J. Schulz, and T. Ziman, J. Phys. A **22**, 511 (1989).
[28] L. G. Caron and C. Bourbonnais, Phys. Rev. B **29**, 4230 (1984).
[29] R. Citro, E. Orignac, and T. Giamarchi, Phys. Rev. B **72**, 024434 (2005).
[30] J. R. Schrieffer and P. A. Wolff, Phys. Rev. **149**, 491 (1966).
[31] I. G. Lang and Y. A. Firsov, Zh. Eksp. Teor. Fiz. **43**, 1843 (1962) [Sov. Phys. JETP **16**, 1301 (1963)].

[32] J. A. M. Vermaseren, math-ph/0010025 (unpublished).
[33] J. A. M. Vermaseren, Nucl. Instrum. Methods Phys. Res. A **559**, 1 (2006).
[34] C. M. Bender and S. A. Orszag, *Advanced Mathematical Methods for Scientists and Engineers: Asymptotic Methods and Perturbation Theory* (Springer, New York, 1999).